

The angular variation of the Biot number $Bi(\theta)$ may be recast as two separate Biot numbers, Bi_u and Bi_f , belonging to the unfinned and finned segments, X_u and X_f , respectively. Therefore, three different weighted-spatial-means of the Biot number Bi_{mean} may be constructed from statistical theory as follows:

The arithmetic-spatial-mean:

$$Bi_a = \frac{X_u Bi_u + X_f Bi_f}{X_u + X_f} \quad (10)$$

The harmonic-spatial-mean:

$$Bi_h = \left[\frac{1}{X_u + X_f} \left(\frac{X_u}{Bi_u} + \frac{X_f}{Bi_f} \right) \right]^{-1} \quad (11)$$

The geometric-spatial-mean:

$$Bi_g = (Bi_u^{X_u} Bi_f^{X_f})^{1/(X_u + X_f)} \quad (12)$$

In light of the foregoing, Eq. (7) becomes separable because \overline{Nu}_{eq} is simply a number. Moreover, the simplicity of Eq. (7) gives rise to an analytical solution that can be readily evaluated by hand or a calculator:

$$\phi_b(\bar{L}) = 1 - \exp(-2\overline{Nu}_{eq}\bar{L}) \quad (13)$$

By choosing various axial stations \bar{L} , the bulk temperatures $\phi_b(\bar{L})$ may be computed immediately from Eq. (13) after an adequate spatial-mean Bi has been selected from the previous list.

Discussion of Results

There are four controlling parameters: 1) N , 2) X_f , 3) Bi_f , and 4) Bi_u . Owing to an abundance of parameters coupled with journal space limitations, only representative results will be given here for two arrays consisting of $N = 4$ and 16 fins. Fixed values of the parameters $X_f = 0.05$, $Bi_f = 50$, and $Bi_u = 1$ have been chosen to conduct the calculations for both arrays. For purposes of comparison, the bulk temperatures based on the three-dimensional distributed model may be regarded as the exact baseline solution. The heat transfer performance will be presented in Figs. 1 and 2 with the bulk temperature ϕ_b along the ordinate and the axial position Z along the abscissa. As expected, the total heat liberation Q_T is enhanced as the number of fins increases.

Without loss of generality, we should anticipate that the exact bulk temperatures based on the three-dimensional distributed model will lie somewhere in between those bulk temperatures calculated with the approximate one-dimensional lumped model. For the one-dimensional model, the data based on the arithmetic-spatial-mean Bi_a are portrayed by circles, whereas those for the geometric-spatial-mean Bi_g are identified by triangles. The curves that are situated in the upper part of each figure are for the one-dimensional model with Bi_a (upper bound), while those in the lower part of the figures are for the Bi_g (lower bound). The importance of the latter rests on its association with the minimum heat removal capabilities of the externally finned tube, say Q_{Tmin} . The results for the harmonic-spatial-mean Bi_h being a weak lower bound are not plotted in the figures in order to preserve clarity.

From an overall appraisal of both figures, it is seen that none of the approximate temperature estimates are very far from those given by the exact temperature predictions. This is an affirmation of the forgiving nature of the discontinuous external convective coefficients $h_e(\theta)$, which are conveniently embedded into the dependable spatial means, h_a and h_g , respectively. The main message of these figures is revealed when overall comparisons are made among the successive set of figures. First, it may be observed that for a sparse array, $N = 4$,

the bulk temperature curve supplied by the one-dimensional model with Bi_g is moderately lower than the exact bulk temperature curve based on the three-dimensional model. It may be observed that the curve of the one-dimensional model is shifted upwards, providing a qualitative statistical estimate. As the number of fins in the array is increased, an approximate symmetrical behavior is noticed and the exact curves are equidistant from the bounding curves. In contrast to the case for $N = 4$, the opposite pattern is in evidence for a dense array of 16 fins. Here, the disparity between the temperature curves of the one-dimensional model with Bi_a and the exact curve of the three-dimensional model is very small. This tendency demonstrates that the curve of the one-dimensional model is shifted downwards, supplying another qualitative statistical estimate. These features elucidated in Figs. 1 and 2 are worthy of note because they put in evidence an intrinsic sweeping behavior attached to the one-dimensional temperature curves.

References

- ¹Mills, A. F., *Heat Transfer*, Irwin, Boston, MA, 1992.
- ²Hausen, H., "Darstellung des Wärmeüberganges in Rohren durch verallgemeinerte Potenzbeziehungen," *Z. VDI Beih. Verfahrenstech.*, No. 4, 1943, pp. 91–95.
- ³Patankar, S. V., *Numerical Heat and Fluid Flow*, Hemisphere, Washington, DC, 1980.

Self-Oscillation Enhancement of Impingement Jet Heat Transfer

R. H. Page,* P. S. Chinnock,† and J. Seyed-Yagoobi‡
Texas A&M University,
College Station, Texas 77843-3123

Introduction

IMPINGING jets are currently widely used in manufacturing and other commercial operations. In some cases it had been found that an oscillation forced on the flow improved the heat transfer, but required auxiliary external power to drive the device that caused the oscillation. Our objective was to produce enhanced heat transfer without an external power source.

Experimental and theoretical studies of transport phenomena augmentation devices that would be useful for retrofitting existing nozzles had been under way at Texas A&M University. The self-oscillating jet impingement nozzle (SOJIN) was developed under the leadership of R. H. Page. It was demonstrated by making a minor addition to a standard in-line jet impingement nozzle. A schematic of the standard in-line jet (ILJ) nozzle and the SOJIN is shown in Fig. 1. The collar is extended over the o.d. of the existing nozzle to a distance where the shear tone frequency is in resonance with the organ pipe frequency of the existing nozzle.^{1–3} A self-oscillation then occurs that has been found to enhance the surface transport phenomena.

Received April 20, 1995; revision received Oct. 30, 1995; accepted for publication Oct. 30, 1995. Copyright © 1995 by the American Institute of Aeronautics and Astronautics, Inc. All rights reserved.

*Professor Emeritus of Mechanical Engineering. Associate Fellow AIAA.

†Graduate Research Assistant, Mechanical Engineering Department.

‡Associate Professor of Mechanical Engineering and Director of Drying Research Center.

Background

The self-oscillating jet was first discovered and documented as a freejet by Hill and Green.⁴ The jet shear layer separated from the constant diameter nozzle exit producing vortices that impinged on the collar lip when the collar was properly extended beyond the pipe exit. This shear-layer impingement provided an oscillation known as a shear-tone. The matching of the shear-tone and the organ pipe frequency of the pipe's finite length resulted in what Hill and Green⁴ called the whistler nozzle. Hasan and Hussain^{5,6} further refined the study of the whistler nozzle. At Texas A&M, the authors decided to use the same general phenomena as a mechanism for enhancing an impinging jet's transport properties. Using airflow, Chinnock³ experimentally studied the surface heat transfer and surface pressure distribution of the SOJIN and compared it to an ILJ nozzle. Flow visualization studies,³ conducted with water flow in a water-filled test section, revealed free transverse wave oscillations and enhanced vortex shedding. Additional airflow visualization studies¹ were carried out using infrared (IR) imaging of CO₂-laced airflow that illustrated the shorter potential core length of the SOJIN compared to the ILJ nozzle.

Results

Nozzles used for this research consisted of a convergence, constant cross section pipe and a collar. Figure 2 illustrates a typical SOJIN configuration. Impingement heat transfer experiments were conducted utilizing the Heat Transfer Jet Impingement Facility (HJIF) at Texas A&M University.⁷ Room temperature air was supplied to the nozzles whose jets im-

pinged on an electrically heated foil. The measurement of the local adiabatic and heated surface temperatures along with the electrical input to the foil enabled calculation of the local heat transfer coefficients during impingement.⁸ Because of the 1-s time constant of the IR thermography system, such surface temperature studies provided time-averaged temperature data and time-averaged heat transfer coefficients.

Figure 3 illustrates typical results of a comparison between the average heat transfer coefficient of a SOJIN with that of an ILJ nozzle. The first-stage oscillation refers to the first audible acoustic oscillation when the collar is extended past the constant diameter exit. The second stage refers to the next distinct mode of oscillation as the collar was further extended.² These results were obtained with tests conducted with a nozzle i.d. of 6.35 mm and a length of 19.05 mm. The nozzles were located three diameters above the impact surface to determine the effect of the self-oscillation on an existing ILJ nozzle. It was readily apparent that the vastly increased vortex shedding of the SOJIN during first-stage oscillation enhanced the average heat transfer coefficient over a large area. An error analysis of the accuracy of the heat transfer coefficient measurements with the HJIF indicated a maximum error of 7%.

Surface pressure measurements for a larger ILJ nozzle and SOJIN are shown in Fig. 4. Both nozzles had an i.d. of 25.4 mm and a length of 76.2 mm. The ILJ nozzle was positioned at six diameters above the impingement surface. This is its optimum height for heat transfer. The SOJIN performed best closer to the surface and was positioned at a height of four

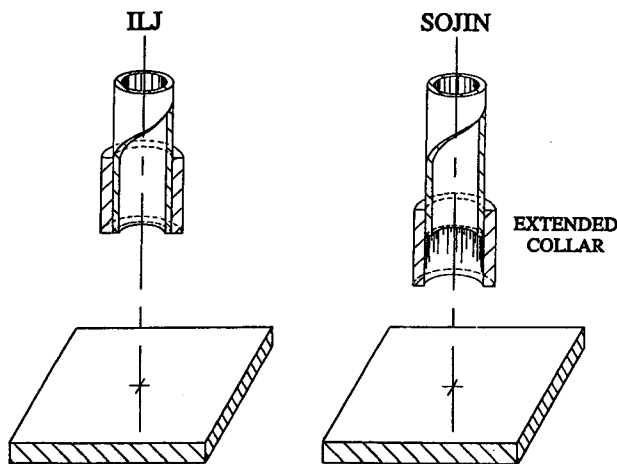


Fig. 1 Schematic of the two nozzles.

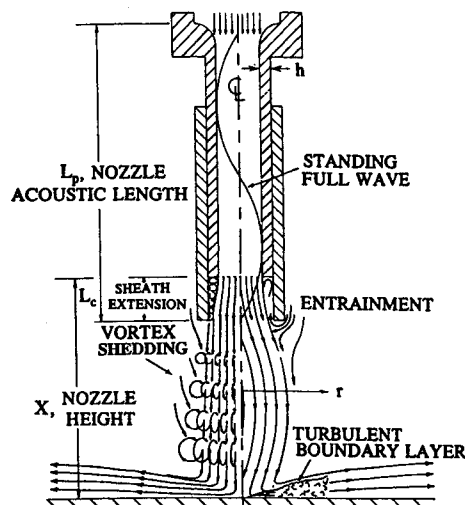


Fig. 2 Sketch of observed SOJIN flow pattern.

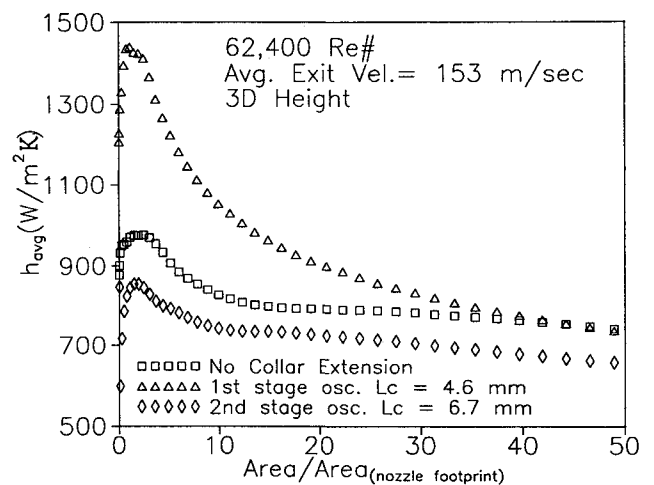


Fig. 3 Average heat transfer coefficient over area of interest ($D = 6.35$ mm).

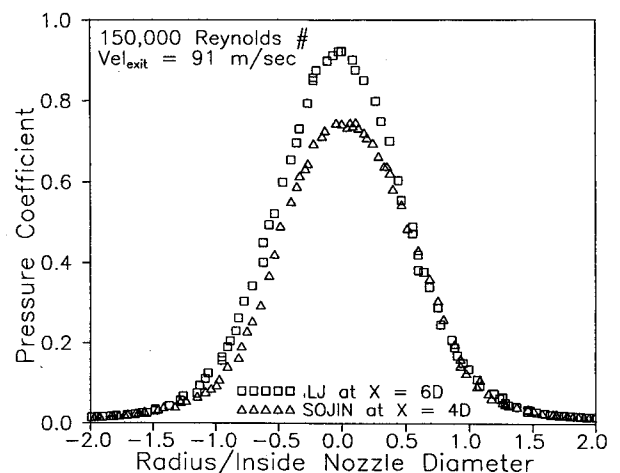


Fig. 4 Surface pressure coefficient of the two nozzles ($D = 25.4$ mm).

diameters. Although the total force on the impingement surface is the same for both nozzles, the SOJIN's higher mixing rate resulted in a lower peak pressure. Also, it was observed that the extended collar of the SOJIN performed like a subsonic diffuser. The pressure ahead of the nozzle dropped slightly when the mass flow was held constant and the operation was changed from standard in-line jet impingement to first-stage oscillation. The second-stage oscillation also decreased the pressure ahead of the nozzle for the same flow rate. Thus, the SOJIN decreases the flow pumping requirements.

Flow visualization studies in a separate experimental facility using a submerged water jet showed vortex shedding during oscillation that came in pulses somewhat similar to those observed by Yokobori et al.⁹ and Crow and Champagne.¹⁰ Acoustic measurements were taken with a decibel meter and a spectrum analyzer. It should be noted that the high-frequency oscillations are audible and advantageous for some situations, but may be objectionable for others. The nozzle used for the experimental results shown in Fig. 3 exhibited first-stage oscillations at 5000 Hz with strong harmonics existing into the ultrasonic range.

Conclusions

A SOJIN has demonstrated higher heat transfer than that of a standard jet nozzle close to a surface. No external power was required and the pumping requirements for the same nozzle mass flow as a standard jet nozzle were slightly reduced. In addition, the SOJIN distributed the pressure increase over the impingement surface area in a less concentrated manner than that of a standard jet impingement nozzle. Thus, inexpensive modifications of industrial systems are possible with the SOJIN, which has untapped application potential.

Acknowledgments

The financial support of the National Science Foundation through Grants CTS-9223640 and CTS-9301287, and the Department of Mechanical Engineering Drying Research Center are gratefully acknowledged.

References

- ¹Chinnock, P. S., and Page, R. H., "Turbulent Heat Transfer with a SOJIN," *ICHMT Proceedings of International Symposium on Turbulence, Heat and Mass Transfer*, Vol. II, Technical Univ. of Lisbon, Portugal, 1994, pp. 15.41–15.46.
- ²Chinnock, P. S., and Page, R. H., "Heat Transfer Enhancement with a Self-Oscillating Jet Impingement Nozzle," *Proceedings of the 10th International Heat Transfer Conference*, Vol. 3, Brighton, England, UK, 1994, pp. 31–36.
- ³Chinnock, P. S., "A Study of the Self-Oscillating Jet Impingement Nozzle (SOJIN)," Drying Research Center, Dept. of Mechanical Engineering, Texas A&M Univ., Rept. DRC 93-1, College Station, TX, Nov. 1993.
- ⁴Hill, W. G., Jr., and Green, P. R., "Increased Turbulent Jet Mixing Rates Obtained by Self-Excited Acoustic Oscillations," *Journal of Fluids Engineering*, Vol. 99, Sept. 1977, pp. 520–525.
- ⁵Hasan, M. A. Z., and Hussain, A. K. M. F., "The Self-Excited Axisymmetric Jet," *Journal of Fluid Mechanics*, Vol. 115, Feb. 1982, pp. 59–89.
- ⁶Hussain, A. K. M. F., and Hasan, M. A. Z., "The 'Whistler-Nozzle' Phenomenon," *Journal of Fluid Mechanics*, Vol. 134, Sept. 1983, pp. 431–458.
- ⁷Page, R. H., Ostowari, C., and Seyed-Yagoobi, J., "Infrared Images of Jet Impingement," *Proceedings of the 20th International Congress on High Speed Photography and Photonics*, Vol. 1801, Society of Photo-Optical Instrumentation Engineers, 1992, pp. 703–709.
- ⁸Page, R. H., Ostowari, C., Seyed-Yagoobi, J., and Gruber, T. C., Jr., "Measurement of Impinging Jet Heat Transfer Utilizing Infrared Techniques," *Experimental Heat Transfer, Fluid Mechanics and Thermodynamics*, Vol. 1, Elsevier, Amsterdam, 1993, pp. 726–732.
- ⁹Yokobori, S., Kasagi, N., Hirata, M., Nakamaru, M., and Hara-maru, Y., "Characteristic Behavior of Turbulence and Transport Phenomena in the Stagnation Region of an Axi-Symmetrical Impinging Jet," *Proceedings of the 2nd Symposium on Turbulent Shear Flows*, Imperial College, London, 1979, pp. 4.12–4.17.
- ¹⁰Crow, S. C., and Champagne, F. H., "Orderly Structure in Jet Turbulence," *Journal of Fluid Mechanics*, Vol. 48, Pt. 3, 1971, pp. 547–591.

Role of Mainstream Flow Velocity in Film Cooling in a Duct

Shyang-Lin Kuo*

General Motors Corporation, Warren, Michigan 48090
and

Neng-Li Zhang† and Wen-Jei Yang‡

University of Michigan, Ann Arbor, Michigan 48109

Introduction

MOST studies on film cooling available in the literature have been found to perform in the subsonic flow region, very few studies were done in the supersonic flow region. Goldstein et al.¹ experimentally studied the film cooling effects in a supersonic flow following a slot. In their work, they used a trip to trigger an oblique shock at a place upstream from the porous section where the mass injection occurred, and studied the film cooling effect from the trailing edge or the porous section to the impingement point of the reflected trip shock. They found that the Mach number was reduced from the boundary-layer trip over the usable portion of the tunnel floor. We believe that the portion of floor where the test data collected was still in the subsonic separated region because of the upstream boundary-layer trip. O'Connor and Haji-Sheikh² numerically studied film cooling by injecting a heated secondary airstream through a rearward-facing slot into a supersonic mainstream with a Mach number of 3.0. The secondary stream was injected with a blowing ratio (secondary-to-main), varying from 0 to 0.328 (Mach numbers of secondary stream were from 0 to 0.986). We noticed that the authors did not extend their studies to have the secondary flow injected across the sonic line (i.e., Mach number of 1). In their studies, the main flow separated because of the slot protruding into the flow region and the inviscid/viscous interaction of flows. A separated flow region was created from the downstream side of the slot to the place where the main flow (compressed shock) reattached. This separated flow was further extended downstream as the blowing rate increased. Notice that this region is essentially dominated by subsonic flow, regardless of its size. From the previous two film cooling studies, a question was raised as to whether the film cooling effect would exist if the secondary flow was injected supersonically into an already supersonic main flow. Since there are not many investigations in supersonic film cooling, the objective of the present work is to explore the causes and the fundamental physics involved in film cooling, especially in the supersonic flow region. The effects of both subsonic and supersonic inlet flows on film cooling is experimentally investigated. A simplified one-dimensional control volume model with mass addition is developed to determine the essential features involved in film cooling.

Received Sept. 19, 1994; revision received Dec. 1, 1995; accepted for publication Dec. 13, 1995. Copyright © 1996 by the American Institute of Aeronautics and Astronautics, Inc. All rights reserved.

*Senior Engineer, Midsize Car Division.

†Professor, Department of Mechanical Engineering and Applied Mechanics. Associate Fellow AIAA.

‡Research Associate, Department of Mechanical Engineering and Applied Mechanics.